

Real-Time Spatial–Temporal Signal Processing With Optical Nonlinearities

Dan M. Marom, *Member, IEEE*, Dmitriy Panasenکو, Pang-Chen Sun, Yuri T. Mazurenko, and Yeshaiahu Fainman, *Senior Member, IEEE*

Abstract—The instantaneous response time of parametric optical nonlinearities enable real-time processing of, and interaction between, spatial and temporal optical waveforms. We review the various signal-processing alternatives based on three- and four-wave-mixing arrangements among spatial and temporal information carrying waveforms. The fast response time of the interaction permits information exchange between the time and space domains, providing the ability to correlate and convolve signals from the two domains. We demonstrate the usefulness of real-time signal processing with optical nonlinearities with the following experiments: converting waveforms from the time to space domain as well as from the space to time domain, spectral phase conjugation and spectral inversion of ultrafast waveforms, transmission of the spatial correlation function on an ultrafast waveform, and a suggestion for a single-shot triple autocorrelation measurement.

Index Terms—Femtosecond pulse shaping, optical information processing, optical signal processing, space-to-time conversion, time reversal, time-to-space conversion, ultrafast processes.

I. INTRODUCTION

HARNESSING ultrashort laser pulse technology for future high-capacity optical communication systems may result in new paradigms for information transmission. Ultrashort pulses can be used as a basis for time-division multiplexing in a fiber communication application, with the potential to carry ultra-high-speed data [1], [2]. The broad spectrum of ultrashort pulses can be utilized as a low-noise multiple-channel optical source for distribution of data using wavelength-division multiplexing by implementing spectral slicing techniques in either the time [3] or the space [4] domain. Data networking applications may benefit from the asynchronous property of code-division multiple access (CDMA), which can be performed by spectrally encoding and decoding ultrashort pulses with unique codes assigned to all users of the network [5], [6]. More sophisticated data modulation formats, such as ultrafast pulse packet transmission on designated time slots [7] and hybrid pulse position modulation with CDMA encoding [8], can result in perfor-

mance gains due to efficient utilization of the ultrashort pulse bandwidth. The ultrafast modulation and detection processes that these techniques require cannot be accomplished by conventional electronic means, due to the limited response time of electronic components, and require novel real-time optical processors based on instantaneous nonlinear phenomena.

During the last few years, we have developed real-time optical processors utilizing nonlinear wave mixing of two or three input waves originating from spatial or temporal channels for synthesizing, processing, and detecting ultrafast waveforms. These devices perform real-time optical signal processing that can be applied to data conversion between slow parallel channels and an ultrafast serial signal. For the data modulation application, we demonstrated a space-to-time mapping processor that converts spatial frequency information from an input spatial channel to the temporal frequency content of an input ultrashort pulse [9], [10]. Using a four-wave-mixing arrangement utilizing cascaded second-order nonlinearities, the output channel yields an ultrafast waveform that is a time-scaled replica of the input spatial image. For detection of ultrafast waveforms, we built a time-to-space mapping processor, which mixes two spatially inverted temporal frequency information waves in a three-wave-mixing arrangement, generating a spatial signal carrying the temporal image for detection by slower electronic means [11], [12]. The two input temporal channels, the first carrying the desired ultrafast information and the second a reference ultrashort pulse, yield a quasi-monochromatic wave due to the mixing process at every point in space between two spectral components that result in a constant carrier frequency (due to the mutually inverted spectra arrangement in the space domain). By introducing only temporal information channels to our processor, we have demonstrated real-time optical processing of temporal waveforms. We performed time-reversal experiments using a four-wave-mixing arrangement with information carrying ultrafast waveform and two reference ultrashort pulses [13]. The time-reversal experiments were based on performing spectral phase conjugation and spectral inversion operations, achieving time reversal of the electrical field and of the complex amplitude waveform, respectively. Spectral phase conjugation is an important feature for compensation of chromatic dispersion and some nonlinear effects of an optical fiber communication link [14].

In this paper, we explore the different real-time signal-processing capabilities that are possible with three- and four-wave-mixing arrangements of spatial and temporal input waveforms. We adopt the methodology for invention introduced by Lohmann [15] to unravel all wave-mixing

Manuscript received January 10, 2001; revised May 14, 2001. This work was supported in part by the National Science Foundation, in part by the Defense Advanced Research Projects Agency, and in part by the U.S. Air Force Office of Scientific Research. The work of D. Marom and D. Panasenکو was supported by the Fannie and John Hertz Foundation.

D. M. Marom was with the Department of Electrical and Computer Engineering, University of California, San Diego, La Jolla, CA 92093-0407 USA. He is now with Bell Laboratories, Lucent Technologies, Holmdel, NJ 07733 USA.

D. Panasenکو, P.-C. Sun, Y. T. Mazurenko, and Y. Fainman are with the Department of Electrical and Computer Engineering, University of California, San Diego, La Jolla, CA 92093-0407 USA.

Publisher Item Identifier S 1077-260X(01)09942-7.

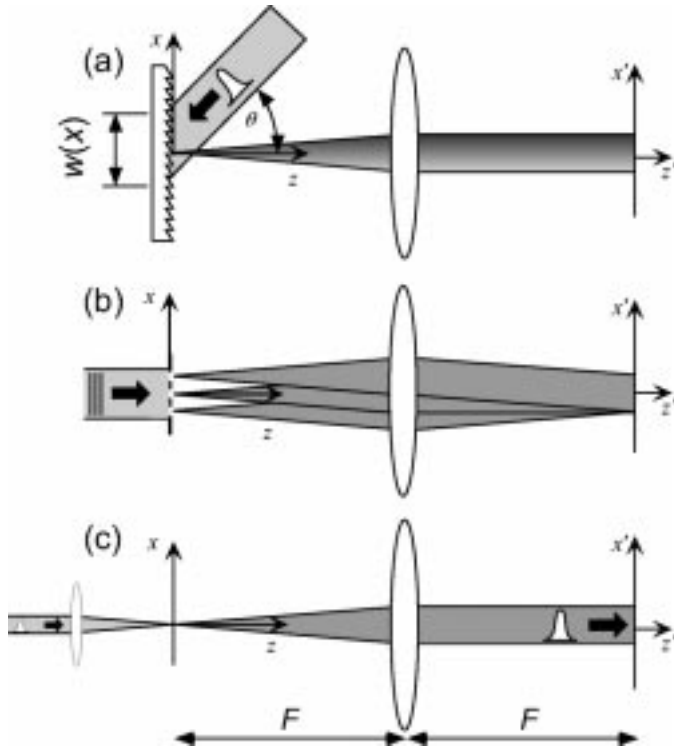


Fig. 1. Input optical waves for consideration in Fourier plane processing. (a) Spectrally decomposed wave, (b) spatial frequency information, and (c) ultrashort pulse.

combinations of the input optical signals. A table is constructed for each interaction type, with columns for the various input waveforms, leading to a unique output signal at each row. We find that this generalized approach describes not only the experiments we have reported but also experiments conducted by others in the past and some new results that are described herein. We demonstrate the transmission of the correlation function of spatial images on an ultrafast waveform and describe a measurement technique of ultrashort pulses that provides the triple correlation values, from which the precise pulse intensity could be extracted.

This paper is organized as follows. Section II defines the input spatial and temporal waves that we consider for interaction via the optical nonlinearities. We limit the scope of this study to interaction at the Fourier plane of a 4-F system, where spatial and temporal frequency information appears. The resulting output waveform combinations in the cases of three- and four-wave mixing are analyzed in Sections III and IV, respectively. New results are described in Sections V and VI, followed by concluding remarks.

II. SPATIAL AND TEMPORAL INPUT WAVES

The spatial and temporal input waves interact by the nonlinear mixing process at the Fourier plane of a 4-F processor. The 4-F arrangement has traditionally been used for coherent processing of spatial images [16] and modified for processing of ultrafast waveforms by introducing diffraction gratings at the input and output planes [17]. The input waves that are to be considered in the wave-mixing processing are (see Fig. 1): 1) spectrally decomposed wave (SDW), i.e., spatially dispersed tem-

poral frequency information; 2) monochromatic wave carrying spatial frequency information; and 3) ultrashort pulse with no spatial information. We assume that all input waves have the same center angular frequency ω_0 . Furthermore, the information contained in the y -axis is omitted, as we consider one-dimensional (1-D) spatial images only and the temporal information is inherently 1-D. We configure the input optical signals with a lateral displacement, for convenience as well as for satisfaction of the noncollinear phase matching requirement. This lateral shift introduces a constant linear phase component in the Fourier plane, which is omitted here for brevity.

The SDW is generated by diffracting the ultrafast waveform signal $p(t)$ from the input plane grating, at an incidence angle θ relative to the grating normal, such that the diffracted wave at the center frequency of the ultrashort pulse is propagating parallel to the optical axis. The field at the back focal plane of the lens, or the Fourier plane, is described by [12]

$$U_{\text{SDW}}(x'; t) = w\left(-\frac{ct}{\alpha}\right) P\left(\frac{x'\omega_0}{\alpha F}\right) \exp\left(j\frac{\omega_0 x'}{\alpha F} t\right) \times \exp(-j\omega_0 t) \quad (1a)$$

where

- $P(\omega)$ temporal Fourier transform of $p(t)$;
- $w(\bullet)$ beam projection profile on the input diffraction grating (or pupil function);
- α grating's angular dispersion parameter ($\alpha = \sin(\theta)$);
- F lens focal length;
- c speed of light in vacuum.

Equation (1a) describes a wave of finite duration (limited by the pupil function), whose transverse profile (along x') carries the temporal spectrum information, with a rotating wave-vector in time. It represents the limiting case of a high-resolution SDW, applicable when the duration of the ultrafast waveform is much shorter than the travel time across the pupil function. In certain signal-processing applications, it is desirable to disperse the spectra in the opposite direction. For this case, we introduce the ultrafast waveform from the opposite side (at angle $-\theta$), utilizing the opposite diffraction order, resulting in the SDW field

$$U_{\text{SDW}}(x'; t) = w\left(\frac{ct}{\alpha}\right) P\left(-\frac{x'\omega_0}{\alpha F}\right) \exp\left(-j\frac{\omega_0 x'}{\alpha F} t\right) \times \exp(-j\omega_0 t). \quad (1b)$$

We assume that the pupil functions of the SDWs of (1a) and (1b) are equal and even functions, resulting in an identical duration and temporal variation for the two functions. Further inspection shows that the temporal frequency information is reversed, as is the wave-vector rotation direction.

The spatial information wave is generated by a 1-D mask $m(x)$ placed at the input plane of the lens and illuminated by a monochromatic light source. At the back focal plane of the lens, we observe the spatial frequency information, given by [16]

$$U_{\text{Spatial}}(x'; t) = M\left(\frac{x'}{\lambda_0 F}\right) \exp(-j\omega_0 t) \quad (2)$$

where $M(f_x)$ is the spatial Fourier transform of the image and λ_0 is the wavelength.

TABLE I
ULTRAFAST SIGNAL-PROCESSING ALTERNATIVES WITH THREE-WAVE MIXING

Input U_1	Input U_2	Resultant U_3	Output signal	Comments
SDW	SDW	SDW with doubled spatial dispersion	Ultrafast waveform: convolution of input waveforms	Output at doubled carrier center frequency
SDW	Inverted SDW	Quasi-monochromatic wave	Spatial signal: correlation of input waveforms	When one input wave is transform limited \rightarrow time-to-space conversion
Spatial frequency wave	Spatial frequency wave	Spatial frequency wave	Spatial signal: convolution of input images	
SDW	Spatial frequency wave	SDW	Ultrafast waveform: correlation of input waveform and spatial image	Output at doubled carrier center frequency
Ultrashort pulse	Ultrashort pulse	Ultrashort pulse	Image of output wave: correlation of input waveforms	Standard intensity cross-correlation measurement
Spatial frequency wave	Ultrashort pulse	Ultrashort pulse	N.A.	Can be used for frequency up-conversion
SDW	Ultrashort pulse	Ultrashort pulse	Image of output wave: convolution of input ultrafast waveforms	Can be used for time-to-space conversion

Finally, we also consider a wave that carries the temporal information directly (as opposed to the temporal frequency information) with no spatial dependence, defined by

$$U_{\text{Temp}}(x'; t) = p(t) \exp(-j\omega_0 t). \quad (3)$$

When this signal is utilized with a real-time nonlinearity, it performs a time gating functionality.

The waves defined in (1)–(3) interact using the parametric processes of a nonlinear crystal. We seek to identify the signal-processing capabilities that are enabled by the ability to generate the product of the waves. For this purpose, the wave-mixing crystal is thin, such that phase mismatch and walkoff effects are not considered. Depending on the combination of input waves, the output signal will be in either the time domain or the space domain. It is further assumed that all waveforms arrive at the processor at the same time (i.e., no time delay between waveforms), unless otherwise noted. In a three-wave-mixing arrangement, the product of the two waves is produced by a noncollinear frequency-sum process. The output wave will be at a doubled carrier frequency. In the four-wave-mixing arrangement, the output is at the same carrier frequency due to the degenerate configuration. We implemented the four-wave mixing by a cascade of three-wave processes; frequency-sum followed by frequency-difference in a noncollinear type-II phase-matching arrangement [18]. In this arrangement, the output signal is copropagating with one of the input signals, but at an orthogonal polarization state. The output signal can be extracted with a polarization beam splitter.

The three-wave-processing capabilities are developed next.

III. ULTRAFAST PROCESSING WITH THREE-WAVE MIXING

In a three-wave-mixing process, two input waves generate a third output wave that is proportional to the product of the two waves, i.e., $U_3 \propto \chi^{(2)} U_1 U_2$. Each of the input fundamental waves U_1 and U_2 can have the form of any one of the three

waves of (1)–(3). Table I summarizes all the fundamental wave combinations and the resulting processing achieved at the output signal.

A. SDW–SDW Mixing

The wave produced by the product of two input fundamental waves of the form of (1a) is given by

$$U_3(x'; t) = w^2 \left(-\frac{ct}{\alpha} \right) P_1 \left(\frac{x'\omega_0}{\alpha F} \right) P_2 \left(\frac{x'\omega_0}{\alpha F} \right) \times \exp \left(j \frac{2\omega_0 x'}{\alpha F} t \right) \exp(-j2\omega_0 t). \quad (4)$$

Applying a spatial Fourier transform to the output plane, with the Fourier kernel adjusted for the new carrier frequency, yields

$$U_{\text{out}}(x''; t) \propto y \left(2 \left(t - \frac{\alpha x''}{c} \right) \right) w^2 \left(-\frac{ct}{\alpha} \right) \exp(-j2\omega_0 t) \quad (5)$$

where $y(t) = p_1(t) \otimes p_2(t)$ and \otimes denotes the convolution operator. The new ultrafast waveform $y(\bullet)$ scans along the output plane at a velocity of c/α . If the signal of (5) is diffracted from a grating with a spatial frequency that is double that of the grating in the input plane of the processor, then the waveform will propagate in free space. The doubled spatial frequency is required since the center wavelength has been halved. The new waveform is proportional to the convolution of the two input waveforms, resulting from the information exchange among the temporal frequency components of $p_1(t)$, $p_2(t)$, and $y(t)$.

B. SDW–Inverted SDW Mixing

The wave produced by the product of two mutually inverted SDW is given by

$$U_3(x'; t) = w \left(-\frac{ct}{\alpha} \right) w \left(\frac{ct}{\alpha} \right) P_1 \left(\frac{x'\omega_0}{\alpha F} \right) P_2 \left(-\frac{x'\omega_0}{\alpha F} \right) \times \exp(-j2\omega_0 t). \quad (6)$$

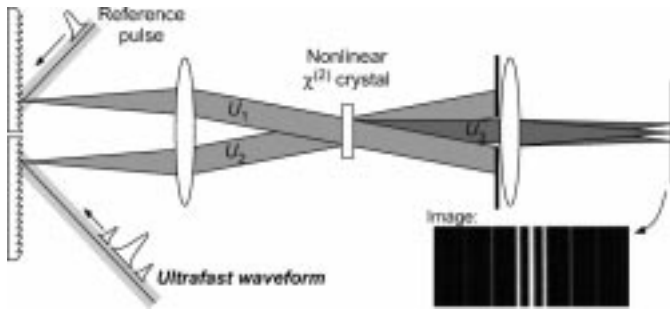


Fig. 2. Experimental setup for time-to-space conversion using mutually inverted spectrally decomposed waves with three-wave mixing. Inset: experimental result showing converted image from an ultrafast pulse sequence. Temporal information can be inferred from image with knowledge of scaling factor.

Applying a spatial Fourier transform, with the Fourier kernel adjusted for the new carrier frequency, yields

$$U_{\text{out}}(x''; t) \propto y\left(-\frac{2\alpha x''}{c}\right) w\left(-\frac{ct}{\alpha}\right) w\left(\frac{ct}{\alpha}\right) \exp(-j2\omega_0 t) \quad (7)$$

where $y(t) = p_1(t) \otimes p_2(-t)$. The stationary spatial signal, $y(\bullet)$, is proportional to the convolution of the two input waveforms, where one of them is reversed in time. This mixing process was developed for time-to-space conversion by using a reference transform-limited pulse for the reversed waveform [11], as illustrated in Fig. 2. We have performed such time-to-space conversions with ultrashort pulses varying in energy levels from subnanjoules (for compatibility with optical communication applications [19]) to millijoules with both LBO and β -barium borate (BBO) crystals, with information conversion efficiencies as high as 120% [12] (the conversion efficiency can exceed 100% due to an equal energy contribution from the reference pulse). The high conversion efficiency is possible due to the favorable phase matching that the mutually inverted SDWs support [20].

C. Mixing Spatial Information Channels

The wave produced by the product of two spatial frequency information channels is given by

$$U_3(x'; t) = M_1\left(\frac{x'}{\lambda_0 F}\right) M_2\left(\frac{x'}{\lambda_0 F}\right) \exp(-j2\omega_0 t). \quad (8)$$

Applying a spatial Fourier transform yields

$$U_{\text{out}}(x''; t) = y(-2x'') \exp(-j2\omega_0 t) \quad (9)$$

where $y(x) = m_1(x) \otimes m_2(x)$. The output spatial signal is a convolution of the input images and is a typical output signal in Fourier optics [16] apart from the scaling factor of two, caused by the frequency doubling. The same signal-processing functionality can be achieved with photorefractive recording media, as the fast response time of the parametric processes is not required here.

D. SDW–Spatial Wave Mixing

The wave produced by the product of a SDW of the form of (1a) and a spatial frequency information wave of the form of (2) is given by

$$U_3(x'; t) = w\left(-\frac{ct}{\alpha}\right) P_1\left(\frac{x'\omega_0}{\alpha F}\right) M_2\left(\frac{x'}{\lambda_0 F}\right) \times \exp\left(j\frac{\omega_0 x'}{\alpha F} t\right) \exp(-j2\omega_0 t). \quad (10)$$

Applying a spatial Fourier transform to the output plane, with the Fourier kernel adjusted for the new carrier frequency, yields

$$U_{\text{out}}(x''; t) \propto y\left(t - \frac{2\alpha x''}{c}\right) w\left(\frac{ct}{\alpha}\right) \exp(-j2\omega_0 t) \quad (11)$$

where $y(t) = p_1(t) \otimes m_2(ct/\alpha)$. The new ultrafast waveform $y(\bullet)$ scans along the output plane at a velocity of $c/2\alpha$. Since both the scanning velocity at the output and the center wavelength have been halved, it is necessary to place a grating with a spatial frequency that is quadruple that of the grating in the input plane of the processor for the waveform to propagate in free space. The new waveform is proportional to the convolution of the input ultrafast waveform and the spatial image, when scaled by c/α to a time-domain variable. Mixing the temporal frequency content of an ultrashort pulse $p_1(t)$ with the spatial frequency information of an image $m_2(x)$ can therefore be used to perform pulse shaping for the output waveform $y(t)$, albeit at a converted wavelength.

E. Mixing Ultrashort Pulses

The wave produced by the product of two ultrashort pulses of the form of (3), while allowing for a timing difference τ between the pulses, is given by

$$U_3(x'; t) = p_1(t)p_2(t + \tau) \exp(-j2\omega_0 t). \quad (12)$$

Suppose next that we place a slow detector at the output of the crystal to measure the intensity of the generated second harmonic light. The instantaneous intensity that is incident on the detector is

$$I_3(x'; t) = |U_3(x'; t)|^2 = |p_1(t)p_2(t + \tau)|^2 = I_1(t)I_2(t + \tau). \quad (13)$$

However, due to the slow response time of detector, the measurement registers the accumulated signal, given by

$$I_3(\tau) = \int I_1(t)I_2(t + \tau) dt. \quad (14)$$

The output signal is the well-known intensity cross-correlation of the ultrafast waveforms, the most fundamental short pulse characterization technique [21], [22]. Note that the intensity cross-correlation signal is observable in space in a noncollinear arrangement (by imaging the output light), but our simplified

TABLE II
ULTRAFAST SIGNAL-PROCESSING ALTERNATIVES WITH FOUR-WAVE MIXING

Input U_1	Input U_2	Input U_3	Resultant U_4	Output signal	Comments
SDW	SDW	SDW	SDW	Ultrafast waveform: convolution and correlation among input waveforms.	Spectral phase conjugation for dispersion compensation
SDW	Inverted SDW	Inverted SDW	SDW	Ultrafast waveform: convolutions among waveform, inverted waveform, and conjugated waveform	True time-inversion for complex amplitude waveforms.
SDW	Spatial frequency wave	Spatial frequency wave	SDW	Ultrafast waveform: convolution and correlation among input waveform and spatial images	Space-to-time conversion when one spatial channel is delta function
Spatial frequency wave	SDW	SDW	Spatial frequency wave	Spatial wave: correlation of temporal waveforms convolved to spatial wave	Time-to-space conversion with dispersion compensation
SDW	Inverted SDW	Spatial frequency wave	Spatial frequency wave	Spatial wave: convolution of temporal waveforms correlated to spatial wave	
Spatial frequency wave	Spatial frequency wave	Spatial frequency wave	Spatial frequency wave	Spatial wave: convolution and correlation among spatial images	
SDW	Ultrashort pulse	Ultrashort pulse	Ultrashort pulse	Spatial image: Intensity triple cross-correlation	Exact waveform can be extracted from triple correlation

representation of (3) does not take into account the space-time dependence of the propagating waveform.

F. Mixing Spatial Waves With Ultrashort Pulses

The wave produced by the product of a spatial frequency information wave and an ultrashort pulse is given by

$$U_3(x';t) = M_1 \left(\frac{x'}{\lambda_0 F} \right) p_2(t) \exp(-j2\omega_0 t). \quad (15)$$

This signal has no significant signal-processing application that comes to mind.

G. SDW-Ultrashort Pulse Mixing

Mixing an SDW with an ultrashort pulse introduces a time gating on the wave, resulting in the output second harmonic wave

$$U_3(x';t) = w \left(-\frac{ct}{\alpha} \right) P_1 \left(\frac{x'\omega_0}{\alpha F} \right) \exp \left(j \frac{\omega_0 x'}{\alpha F} t \right) p_2(t) \times \exp(-j2\omega_0 t). \quad (16)$$

Applying a spatial Fourier transform to the output plane, with the Fourier kernel adjusted for the new carrier frequency, yields

$$U_{\text{out}}(x'';t) \propto p_1 \left(t - \frac{2\alpha x''}{c} \right) p_2(t) w \left(-\frac{ct}{\alpha} \right) \exp(-j2\omega_0 t). \quad (17)$$

We wish to record the output spatial signal by placing a sensing device that integrates the output intensity, such as a charge-coupled device (CCD) camera. The observed image is given by

$$I_{\text{out}}(x'') = \int |U_{\text{out}}(x'';t)|^2 dt \approx \int I_1 \left(t - \frac{2\alpha x''}{c} \right) I_2(t) dt \quad (18)$$

where we assumed that the long aperture duration is negligible due to the short duration of the ultrafast waveforms (consistent with our assumption of a high-resolution SDW). The image corresponds to the intensity cross-correlation of the two ultrafast waveforms, converted to the space domain and permitting single-shot measurement. This approach was used for one of the earliest experiments demonstrating time-to-space conversion, albeit with a slower excitonic nonlinear process in a ZnSe film [23]. It is also possible to perform the time-to-space conversion by placing the nonlinear crystal at the image plane of the grating instead of at the Fourier plane, as recently demonstrated [24].

IV. ULTRAFAST PROCESSING WITH FOUR-WAVE MIXING

In a degenerate four-wave-mixing process, three input waves at the same carrier frequency generate a fourth output wave that is proportional to $U_4 \propto \chi^{(3)} U_1 U_2 U_3^*$. The output wave is also at the same carrier frequency as the input waves. Each of the input fundamental waves U_1 , U_2 , and U_3 can have the form of any one of the three waves defined by (1)–(3). Table II summarizes the input wave combinations of interest and the resulting processing achieved at the output signal.

A. SDW Mixing

The wave produced by the three input fundamental waves of the form of (1a) is given by

$$U_4(x';t) = w^3 \left(-\frac{ct}{\alpha} \right) P_1 \left(\frac{x'\omega_0}{\alpha F} \right) P_2 \left(\frac{x'\omega_0}{\alpha F} \right) P_3^* \left(\frac{x'\omega_0}{\alpha F} \right) \times \exp \left(j \frac{\omega_0 x'}{\alpha F} t \right) \exp(-j\omega_0 t). \quad (19)$$

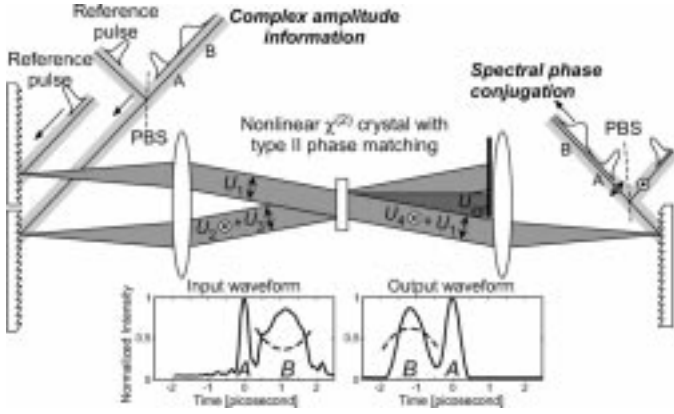


Fig. 3. Experimental setup for time reversal using spectral phase conjugation with four-wave mixing. Inset: experimental result showing time reversal of pulses A and B and chirp flipping (dashed line corresponds to simulated phase function).

Applying a spatial Fourier transform yields

$$U_{\text{out}}(x''; t) \propto y\left(t - \frac{\alpha x''}{c}\right) w^3\left(\frac{ct}{\alpha}\right) \exp(-j\omega_0 t) \quad (20)$$

where $y(t) = p_1(t) \otimes p_2(t) \otimes p_3^*(-t) = p_1(t) \otimes p_2(t) \star p_3(t)$ and \star denotes the correlation operation. The new ultrafast waveform $y(\bullet)$ scans along the output plane at a velocity of $-c/\alpha$ and can be coupled to free-space propagation by diffraction from a grating identical to the grating at the input plane of the processor. The new waveform is proportional to the convolution of the first and second input waveforms with the third waveform, which is time-reversed and conjugated. A convolution with the time-reversed and conjugated signal is equivalent to a correlation operation. Thus, the output waveform is a combination of a convolution and correlation among the input waveforms. If $p_1(t)$ and $p_2(t)$ are both transform-limited pulses, the output spectra is a phase conjugate of the spectra of $p_3(t)$, which is an important application for dispersion compensation in optical fiber communication links. We have performed the spectral phase conjugation experiment (see Fig. 3) with a signal wave consisting of a pulse pair: a chirped pulse followed by a transform limited pulse [13]. As expected, the two pulses exchanged location, while the chirped pulse also reversed its chirp sign. All pulses were obtained from a millijoule source pulse and processed in a BBO crystal with cascaded second-order nonlinearities.

B. SDW and Inverted SDW Mixing

There are several options for choosing which channels to introduce to the processor from the opposite side, such that their corresponding SDW will be inverted. When the SDWs of waves U_2 and U_3 are inverted, the wave produced by the three input fundamental waves is given by

$$U_4(x'; t) = w\left(-\frac{ct}{\alpha}\right) w^2\left(\frac{ct}{\alpha}\right) P_1\left(\frac{x'\omega_0}{\alpha F}\right) P_2\left(-\frac{x'\omega_0}{\alpha F}\right) \times P_3^*\left(-\frac{x'\omega_0}{\alpha F}\right) \exp\left(j\frac{\omega_0 x'}{\alpha F} t\right) \exp(-j\omega_0 t). \quad (21)$$

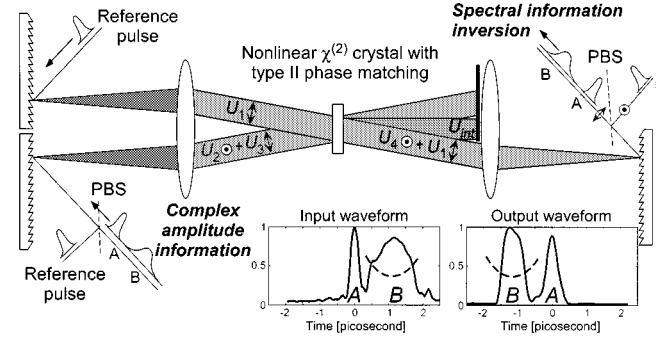


Fig. 4. Experimental setup for time reversal using spectral inversion with four-wave mixing. Inset: experimental result showing time reversal of pulses A and B and preservation of chirp sign (dashed line corresponds to simulated phase function).

Applying a spatial Fourier transform yields

$$U_{\text{out}}(x''; t) \propto y\left(t - \frac{\alpha x''}{c}\right) w\left(-\frac{ct}{\alpha}\right) w^2\left(\frac{ct}{\alpha}\right) \exp(-j\omega_0 t) \quad (22)$$

where $y(t) = p_1(t) \otimes p_2(-t) \otimes p_3^*(t) = p_1(t) \otimes p_2(-t) \star p_3(-t)$. The unique feature of this arrangement is that the output waveform is proportional to the time-reversed complex amplitude waveform of the second channel. We have demonstrated this property for the first time [13], to the best of our knowledge, by using transform-limited pulses for $p_1(t)$ and $p_2(t)$. The signal wave consisted of a pulse pair: a chirped pulse followed by a transform-limited pulse. As expected, the two pulses exchanged location, while the chirped pulse preserved its chirp sign (see Fig. 4).

C. SDW and Spatial Wave Mixing I

The wave produced by the interaction of an SDW with two spatial frequency information waves is given by

$$U_4(x'; t) = w\left(-\frac{ct}{\alpha}\right) P_1\left(\frac{x'\omega_0}{\alpha F}\right) M_2\left(\frac{x'}{\lambda_0 F}\right) M_3^*\left(\frac{x'}{\lambda_0 F}\right) \times \exp\left(j\frac{\omega_0 x'}{\alpha F} t\right) \exp(-j\omega_0 t). \quad (23)$$

Applying a spatial Fourier transform yields

$$U_{\text{out}}(x''; t) \propto y\left(t - \frac{\alpha x''}{c}\right) w\left(-\frac{ct}{\alpha}\right) \exp(-j\omega_0 t) \quad (24)$$

where $y(t) = p_1(t) \otimes m_2(ct/\alpha) \otimes m_3^*(-ct/\alpha) = p_1(t) \otimes m_2(ct/\alpha) \star m_3(ct/\alpha)$. The output ultrafast waveform carries the correlation information of the two spatial channels. Such a configuration can be useful for performing a spatial correlation function and transmitting the correlation information to a remote site on a temporal channel. The spatial correlation feature was demonstrated and is discussed in Section V. When one of the spatial channels is a delta function, the result is a space-to-time conversion [9], [10] (see Fig. 5). All the input optical signals were generated from a single millijoule source

pulse; the pulse was stretched with a grating pair for implementing the two monochromatic spatial channels.

D. SDW and Spatial Wave Mixing II

A different arrangement of the input interacting waves produces the equivalent of real-time time-to-space conversion, similar to that achieved with spectral holography [25]. The wave produced by the interaction of a spatial wave with two SDWs is given by

$$U_4(x'; t) = w^2 \left(-\frac{ct}{\alpha} \right) M_1 \left(\frac{x'}{\lambda_0 F} \right) P_2 \left(\frac{x' \omega_0}{\alpha F} \right) P_3^* \left(\frac{x' \omega_0}{\alpha F} \right) \times \exp(-j\omega_0 t). \quad (25)$$

Applying a spatial Fourier transform yields

$$U_{out}(x''; t) \propto y(-x'') w^2 \left(-\frac{ct}{\alpha} \right) \exp(-j\omega_0 t) \quad (26)$$

where $y(x) = m_1(x) \otimes p_2(\alpha x/c) \star p_3(\alpha x/c)$. The stationary output signal carries the information of the correlation of the two waveforms, scaled to a spatial dependence, convolved with the spatial signal. Such a configuration can be useful for dispersion cancellation when two waveforms are transmitted along the same path [7]. When the input spatial signal carries no information (delta function), the output signal results in a time-to-space conversion by four-wave mixing, achieving the same result as holographic four-wave mixing, albeit in real-time.

E. SDW, Inverted SDW, and Spatial Wave Mixing

It is possible to mix SDW and get a spatial output by wave mixing an SDW, an inverted SDW, and a spatial frequency information wave. The resulting wave is given by

$$U_4(x'; t) = w \left(-\frac{ct}{\alpha} \right) w \left(\frac{ct}{\alpha} \right) P_1 \left(\frac{x' \omega_0}{\alpha F} \right) P_2 \left(-\frac{x' \omega_0}{\alpha F} \right) \times M_3^* \left(\frac{x'}{\lambda_0 F} \right) \exp(-j\omega_0 t). \quad (27)$$

Applying a spatial Fourier transform yields

$$U_{out}(x''; t) \propto y \left(-\frac{\alpha x''}{c} \right) w \left(-\frac{ct}{\alpha} \right) w \left(\frac{ct}{\alpha} \right) \exp(-j\omega_0 t) \quad (28)$$

where $y(t) = p_1(t) \otimes p_2(-t) \otimes m_3^*(-ct/\alpha) = p_1(t) \otimes p_2(-t) \star m_3(ct/\alpha)$. The stationary output signal carries the information of the convolution of the two waveforms (where one is reversed in time) and a correlation with the spatial signal. Such a configuration can be useful to correlate an incoming waveform $p_1(t)$ with a spatial image and requiring a spatial output for subsequent detection (by using a featureless reference pulse for the second temporal channel).

F. Spatial Wave Mixing

Three spatial frequency information waves interacting via degenerate four-wave mixing generate an output wave given by

$$U_4(x'; t) = M_1 \left(\frac{x'}{\lambda_0 F} \right) M_2 \left(\frac{x'}{\lambda_0 F} \right) M_3^* \left(\frac{x'}{\lambda_0 F} \right) \times \exp(-j\omega_0 t). \quad (29)$$

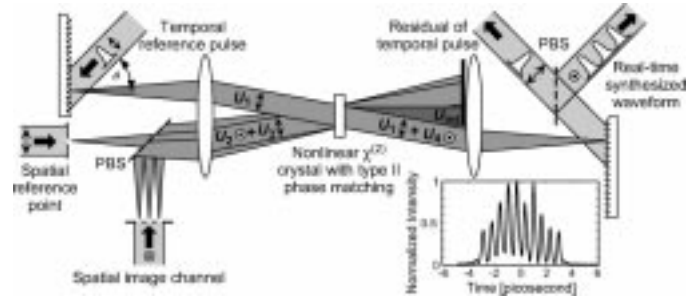


Fig. 5. Experimental setup for space-to-time conversion with four-wave mixing. Inset: experimental result showing conversion of spatial information (regularly placed slits) to an ultrafast waveform consisting of a pulse sequence at 1.56-THz repetition rate.

Applying a spatial Fourier transform yields

$$U_{out}(x''; t) = y(-x'') \exp(-j\omega_0 t) \quad (30)$$

where $y(x) = m_1(x) \otimes m_2(x) \otimes m_3^*(x) = m_1(x) \otimes m_2(x) \star m_3(x)$. The convolution and correlation relationship among the input spatial images is typical in holographic signal processing. Utilizing nonlinear wave mixing yields the same results in real time.

G. SDW and Ultrashort Pulse Mixing

A time-delay parameter is added to one of the ultrashort pulses for describing the interaction of an SDW with two ultrashort pulses. The output wave is therefore given by

$$U_4(x'; t) = w \left(-\frac{ct}{\alpha} \right) P_1 \left(\frac{x' \omega_0}{\alpha F} \right) \exp \left(j \frac{\omega_0 x'}{\alpha F} t \right) \times p_2(t) p_3^*(t - t_0) \exp(-j\omega_0 t). \quad (31)$$

Applying a spatial Fourier transform yields

$$U_{out}(x''; t) = w \left(-\frac{ct}{\alpha} \right) p_1 \left(t - \frac{\alpha x''}{c} \right) p_2(t) p_3^*(t - t_0) \times \exp(-j\omega_0 t). \quad (32)$$

The observed image on a slow detection device such as a film or camera is described by

$$S_{out}(x''; t_0) = \int_{-\infty}^{\infty} |U_{out}(x''; t)|^2 dt \approx w^2(0) \int_{-\infty}^{\infty} I_1 \left(t - \frac{\alpha x''}{c} \right) I_2(t) I_3(t - t_0) dt \quad (33)$$

where we used the approximation that the field strength variation due to the spatial beam mode does not change for the short duration of the sampling pulse. The image contains the triple cross-correlation information of the three input ultrashort waveform intensities. The triple correlation requires two time-lag parameters. In the result of (33), one time-lag parameter is mapped to the spatial domain, while the other is set by the relative time delay between the second and third ultrafast waveforms. If all the input waveforms to the processor are identical, then the triple autocorrelation data can be used to extract the exact intensity profile of the input short pulse. To reconstruct the input waveform intensity profile, the complete two-dimensional (2-D) cor-

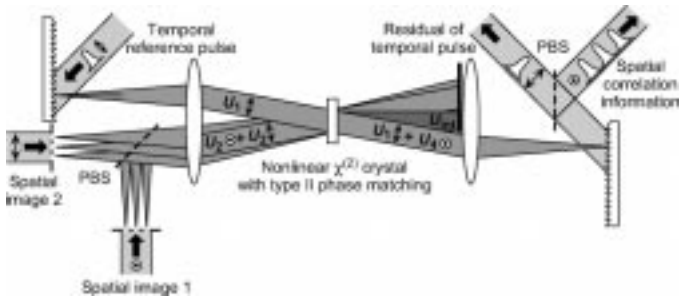


Fig. 6. Experimental setup for the information exchange among two input spatial channels and an input ultrafast waveform. The output ultrafast waveform contains the correlation information of the two spatial channels.

relation matrix is required [26]. Using this arrangement would require a sequence of measurements, varying the parameter t_0 for each measurement. A single-shot variant of this technique is described in Section VI.

V. SPATIAL CORRELATION FUNCTION CARRIED ON AN ULTRAFAST WAVEFORM

Mixing spectrally decomposed waves and spatially Fourier transformed images results in an information exchange between the temporal spectra of the ultrashort pulse and the spatial spectra of the image. The information exchange results in waveform synthesis by a space-to-time conversion. A three-wave-mixing arrangement for the information exchange results in a temporal signal with a doubled center frequency. When the synthesized waveform is required to have an identical center frequency, a degenerate four-wave-mixing arrangement is utilized, with a second spatial signal consisting of a (featureless) point source. In this section, the information exchange between the two spatial images and the ultrafast waveform is demonstrated (see Fig. 6).

Mixing an SDW and two spatially Fourier transformed images using a degenerate four-wave-mixing process results in an output temporal waveform that is a convolution of the input temporal waveform with the correlation of the two spatial images, properly scaled to a time-domain representation, i.e., $y(t) = p_1(t) \otimes m_2(ct/\alpha) * m_3(ct/\alpha)$. In the experiments, a commercial laser system consisting of a Ti:Sapphire ultrashort pulse oscillator and a regenerative amplifier was used. The system generates ultrashort laser pulses of 100 fs duration at a center wavelength of 800 nm with an energy level of 1 mJ per pulse. Ninety percent of the emitted output pulse power was utilized for the intense quasi-monochromatic light source required by the spatial channels and stretched to a duration of several picoseconds by a grating pair. The stretched pulse was split into two beams for implementing the two quasi-monochromatic spatial channels. The remaining 10% of the short pulse laser output power was used as the reference ultrashort pulse in the input temporal channel. The SDW U_1 is generated by a 600-lines/mm blazed grating that provides an angular dispersion parameter of $\alpha = 0.48$ and a lens of $F = 375$ mm focal length. The four-wave mixing is performed by cascaded second-order nonlinearities in a 2-mm-long type-II BBO crystal. Several experiments were conducted to illustrate this real-time spatial-temporal processing technique. All the output waveforms were observed with a time-to-space

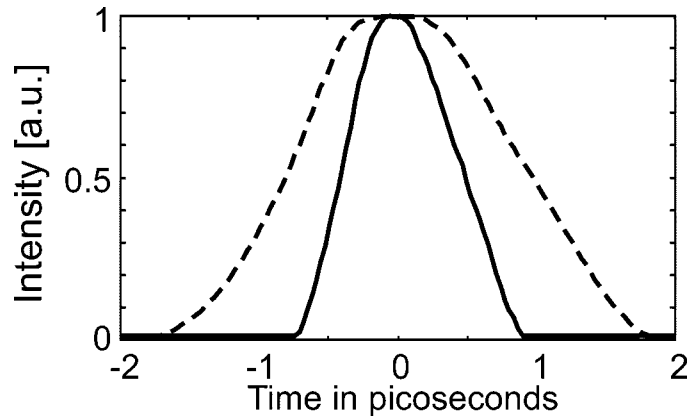


Fig. 7. Ultrafast waveforms containing the correlation information of two rectangular apertures in the spatial domain. Solid curve: ultrafast waveform from two narrow rectangular spatial signals of identical width. Dashed curve: wider, unequal rectangular spatial signals, resulting in a trapezoid correlation function.

converter based on three-wave mixing with mutually inverted SDW. The reference pulse source required for the pulse imager was the residual input pulse of the spatial-temporal processor, after separating it from the output waveform with a polarizing beam splitter. The output signal's intensity was viewed with a CCD camera, and the temporal information was extracted from the image.

The first experiment consisted of placing two variable slits in the spatial channels, implementing a rectangular spatial distribution. The correlation function of two rectangular signals has a trapezoidal shape; the plateau is observed for correlation delays smaller than the width of the narrower rectangle. When the two rectangles are of identical width, the correlation function is triangular. If the width of one of the rectangles is very small (approaching a point source), then the output signal will result in a space-to-time conversion and resemble a square pulse (generation of square pulses using this technique reported in [10]). The ultrafast output waveform will contain smoothed features due to the convolution operation with the input ultrashort pulse. Additional smoothing is performed in the waveform imaging operation. The experimental results of Fig. 7 precisely illustrate the correlation function of rectangular signals described above. A triangular pulse shape was observed for equal rectangular widths (solid curve), while a trapezoidal pulse shape was observed for unequal rectangular widths (dashed curve).

A second experiment was performed with spatial channels that are coded with pseudorandom masks. The phase mask (for implementing values of ± 1) was prepared by wet-etching the spatial information into a quartz substrate. The spatial information consisted of contiguous equal-width rectangular sections (each $75 \mu\text{m}$) encoded with transmission values of ± 1 according to a 127 maximal length sequence [see Fig. 8(a)]. The maximal length sequence was chosen for the low correlation values it exhibits for any delay other than zero. When the mask was placed in one spatial channel and the second consisted of a point source, a space-to-time conversion was performed and the resulting waveform appeared random [see Fig. 8(b)]. When both spatial channels had an identical mask, a correlation peak at the zero delay location appeared [see Fig. 8(c)]. At other

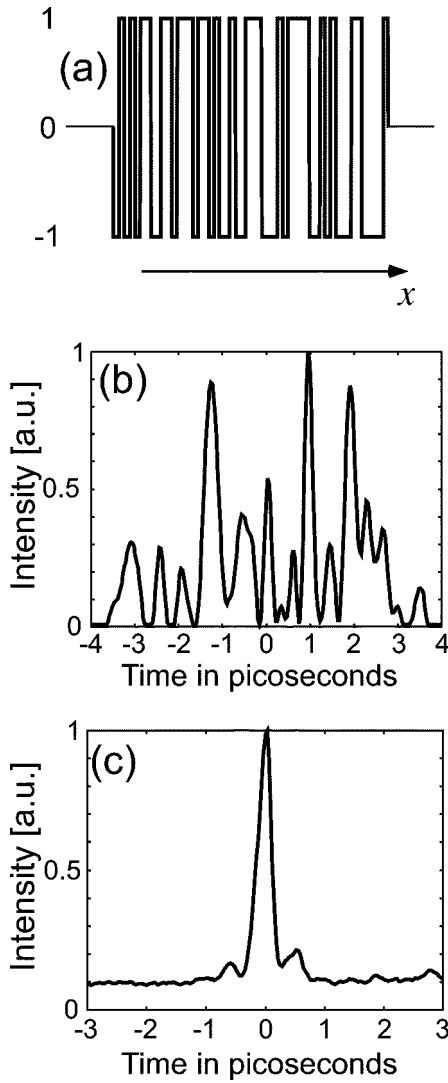


Fig. 8. Ultrafast spatial-temporal processing with pseudorandom information. (a) Maximal length sequence used for spatial mask information. (b) Synthesized space-to-time conversion signal from mask using a point source for second channel. (c) Correlation function of two identical masks carried on a temporal waveform.

delay times, the ultrafast waveform had a small signal from the nonzero correlation values.

This type of processor can be used for transmitting spatial correlation information via a temporal channel. Such capability may be important for transmission of information from a hostile environment for detection at a safer location.

VI. SINGLE-SHOT IMPLEMENTATION OF THE TRIPLE AUTOCORRELATION

Wave mixing an SDW and two ultrashort pulses resulted in an output plane image that contained some of the triple correlation values, as developed in Section IV. For reconstruction of the original intensity profile of the ultrashort pulse, the entire correlation matrix is required. Therefore, a sequence of measurements is necessary to fully characterize the ultrashort pulse intensity. The parameter that is changed between subsequent measurements is the relative time delay between the two ultrashort

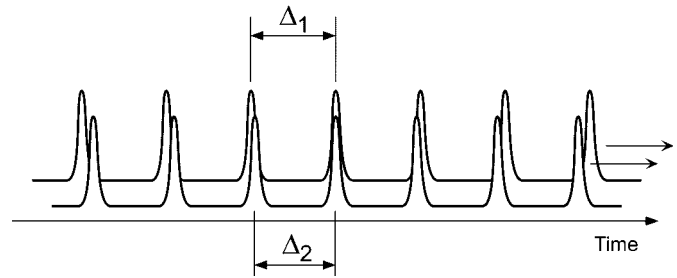


Fig. 9. Ultrashort pulse trains with different periods to generate a single-shot triple correlation measurement.

pulses. In this section, a single-shot technique based on ultrashort pulse trains for sampling the SDW is described.

We modify the technique described above by using two ultrashort pulse trains instead of the two ultrashort pulses. Generating a pulse train of identical ultrashort pulses is possible with waveform synthesis techniques. Additionally, all pulses are assumed to have an identical waveform. The period between consecutive pulses is different for the two pulse trains. Let one pulse train have pulse separation of Δ_1 and the other Δ_2 , and let $\Delta_1 \approx \Delta_2$ (see Fig. 9). The resulting output field is given by [see (32)]

$$U_{\text{out}}(x''; t) = w\left(-\frac{ct}{\alpha}\right) p\left(t - \frac{\alpha x''}{c}\right) \left(\sum_n p(t - n\Delta_1)\right) \times \left(\sum_m p^*(t - m\Delta_2)\right) \exp(-j\omega_0 t). \quad (34)$$

Since the pulse separations Δ_1 and Δ_2 are nearly equal, U_{out} will be zero if $n \neq m$. Therefore, we can rewrite (34) as

$$U_{\text{out}}(x''; t) = \sum_n w\left(-\frac{ct}{\alpha}\right) p\left(t - \frac{\alpha x''}{c}\right) p(t - n\Delta_1) \times p^*(t - n\Delta_2) \exp(-j\omega_0 t). \quad (35)$$

The observed image on a slow detection device such as a film or camera is then described by

$$S_{\text{out}}(x'') = \int_{-\infty}^{\infty} |U_{\text{out}}(x''; t)|^2 dt = \int_{-\infty}^{\infty} \left(\sum_n w\left(-\frac{ct}{\alpha}\right) p\left(t - \frac{\alpha x''}{c}\right) \times p(t - n\Delta_1) p^*(t - n\Delta_2)\right) \times \left(\sum_k w\left(-\frac{ct}{\alpha}\right) p^*\left(t - \frac{\alpha x''}{c}\right) \times p^*(t - k\Delta_1) p(t - k\Delta_2)\right) dt. \quad (36)$$

Again, since the pulse separations Δ_1 and Δ_2 are nearly equal, S_{out} will be zero if $n \neq k$. Therefore

$$\begin{aligned} S_{\text{out}}(x'') &= \sum_n \int_{-\infty}^{\infty} w^2 \left(-\frac{ct}{\alpha} \right) I \left(t - \frac{\alpha x''}{c} \right) I(t - n\Delta_1) \\ &\quad \times I(t - n\Delta_2) dt \\ &\approx \sum_n w^2 \left(-\frac{cn\Delta_1}{\alpha} \right) \int_{-\infty}^{\infty} I \left(t - \frac{\alpha x''}{c} \right) \\ &\quad \times I(t - n\Delta_1) I(t - n\Delta_2) dt \end{aligned} \quad (37)$$

where we used the approximation that the field strength variation due to the spatial beam mode does not change for the short duration of each sampling pulse at time $t = n\Delta_1$. Let us assume that $\Delta_2 = \Delta_1 + \varepsilon$. Additionally, with a change of integration variable, (37) can be rewritten as

$$\begin{aligned} S_{\text{out}}(x'') &\approx \sum_n w^2 \left(-\frac{cn\Delta_1}{\alpha} \right) \int_{-\infty}^{\infty} I \left(\xi + n\Delta_1 - \frac{\alpha x''}{c} \right) \\ &\quad \times I(\xi) I(\xi - n\varepsilon) dt. \end{aligned} \quad (38)$$

The integral in (38) is now identifiable as the triple autocorrelation integral, where one lag parameter is mapped to the spatial domain while the second lag parameter is $n\varepsilon$. Each order of n is mapped to a different location on the spatial output (centered at $x'' = cn\Delta_1/\alpha$) and is associated with the lag $n\varepsilon$. Therefore, the triple correlation matrix values are raster scanned on the 1-D output space. Each order n is also scaled by the input pupil function. This effect can be accounted for by measuring the profile and normalizing the measurement or by ensuring that the mode is uniform. After collecting the 1-D correlation values and assembling the matrix, an algorithm can be applied to find the exact intensity profile of the ultrashort pulse. The sampling method described here can be associated with bandwidth adaptation techniques [27], where a 2-D distribution is converted to a 1-D distribution. Such bandwidth adaptation techniques have also been applied to time-to-2-D space and 2-D space-to-time conversions [28].

VII. DISCUSSION AND CONCLUSION

We have examined the different signal-processing capabilities that are enabled when spatial and temporal information bearing waves interact via fast parametric processes. The methodical process of investigating all the input wave combinations describes the experiments we have conducted in the past and reveals new options for processing of ultrafast data. These techniques can be used for synthesis, processing, and detection of ultrafast waveforms. Such capabilities may be utilized in future high-capacity communication systems, ultrafast optical computation, and scientific uses in investigation of ultrafast phenomena and quantum control.

As our analysis showed, there are many methods one may choose for conversion of data from the time-to-space domain: time-domain noncollinear arrangement, mixing the time domain with the SDW (or at the image plane of the grating), and mixing two mutually inverted SDWs. All methods generate the

intensity cross-correlation signal with a reference transform limited pulse [compare (18) and the intensity of (7), for example]. The different arrangements offer functional trade-offs among time window of apparatus, phase matching, and walkoff effects; crystal (or interaction) length; and conversion efficiency. However, it was not within the scope of this paper to analyze which technique offers the best performance for a given set of constraints.

The instantaneous nature of wave-mixing processes for information conversion from the spatial domain to the temporal domain is best utilized when the spatial information channel is rapidly changing. In our analysis, we have assumed that the spatial information is stationary with respect to the temporal channel time window. This could be accomplished by a 1-D fiber array, which supplies synchronized parallel data streams (for such telecom-oriented applications, the wave-mixing process has to be optimized for the expected low power levels). If the spatial channel information changes during the time window of the spectral processor, the output signal will exhibit different temporal information across its transverse extent. It should be noted that when the spatial information is varying at slow rates, alternative Fourier plane processing elements such as photorefractives may be employed (spectral holography [29]).

Ultrafast waveform synthesis by space-to-time conversion can be performed by three- and four-wave-mixing arrangements. The degenerate four-wave-mixing arrangement is the more useful option, as it is usually desirable to modify an input ultrashort pulse to a prescribed waveform without a center frequency shift. However, since all the processing is performed by real-time parametric interaction, it is possible to add a wavelength-tuning feature. When utilizing the four-wave-mixing process with tunable lasers for implementation of the spatial channels, the center frequency of the synthesized waveform will be shifted by the frequency difference of the two spatial lasers, in accordance with the energy conservation principle.

REFERENCES

- [1] V. W. S. Chan, K. L. Hall, E. Modiano, and K. A. Rauschenbach, "Architectures and technologies for high-speed optical data networks," *J. Lightwave Technol.*, vol. 16, pp. 2146–68, 1998.
- [2] M. Nakazawa, E. Yoshida, T. Yamamoto, E. Yamada, and A. Sahara, "TDM single channel 640 Gbit/s transmission experiment over 60 km using 400 fs pulse train and walk-off free, dispersion flattened nonlinear optical loop mirror," *Electron. Lett.*, vol. 34, pp. 907–908, 1998.
- [3] M. C. Nuss, W. H. Knox, and U. Koren, "Scalable 32 channel chirped-pulse WDM source," *Electron. Lett.*, vol. 32, pp. 1311–12, 1996.
- [4] E. A. De Souza, M. C. Nuss, W. H. Knox, and D. A. B. Miller, "Wavelength division multiplexing with femtosecond pulses," *Opt. Lett.*, vol. 20, pp. 1166–1168, 1995.
- [5] A. M. Weiner, J. P. Heritage, and J. A. Salehi, "Encoding and decoding of femtosecond pulses," *Opt. Lett.*, vol. 13, pp. 300–302, 1988.
- [6] J. A. Salehi, A. M. Weiner, and J. P. Heritage, "Coherent ultrashort light pulse code-division multiple access communication systems," *J. Lightwave Technol.*, vol. 8, pp. 478–491, 1990.
- [7] D. M. Marom, P.-C. Sun, and Y. Fainman, "Analysis of spatial-temporal converters for all-optical communication links," *Appl. Opt.*, vol. 37, pp. 2858–2868, 1998.
- [8] K.-S. Kim, D. M. Marom, L. B. Milstein, and Y. Fainman, "Hybrid pulse position modulation/ultrashort light pulse code division multiple access," *IEEE Trans. Commun.*, submitted for publication.
- [9] D. M. Marom, D. Panasencko, P.-C. Sun, and Y. Fainman, "Spatial-temporal wave mixing for space-time conversion," *Opt. Lett.*, vol. 24, pp. 563–565, 1999.

- [10] D. Marom, D. Panasenکو, P.-C. Sun, and Y. Fainman, "Femtosecond-rate space-to-time conversion," *J. Opt. Soc. Amer. B*, vol. 17, pp. 1759–1773, 2000.
- [11] P. C. Sun, Y. T. Mazurenko, and Y. Fainman, "Femtosecond pulse imaging: Ultrafast optical oscilloscope," *J. Opt. Soc. Amer. A*, vol. 14, pp. 1159–1170, 1997.
- [12] D. M. Marom, D. M. Panasenکو, P.-C. Sun, and Y. Fainman, "Linear and nonlinear operation of a time-to-space processor," *J. Opt. Soc. Amer. A*, vol. 18, pp. 448–458, 2001.
- [13] D. Marom, D. Panasenکو, R. Rokitski, S. Pang-Chen, and Y. Fainman, "Time reversal of ultrafast waveforms by wave mixing of spectrally decomposed waves," *Opt. Lett.*, vol. 25, pp. 132–134, 2000.
- [14] A. Yariv, D. Fekete, and D. M. Pepper, "Compensation for channel dispersion by nonlinear optical phase conjugation," *Opt. Lett.*, vol. 4, pp. 52–54, 1979.
- [15] A. W. Lohmann, "Teaching how to invent—Is it possible?," *Israel J. Technol.*, vol. 18, pp. 214–217, 1980.
- [16] J. W. Goodman, *Introduction to Fourier Optics*, 2nd ed. New York: McGraw-Hill, 1996.
- [17] C. Froehly, B. Colombeau, and M. Vampouille, "Shaping and analysis of picosecond light pulses," in *Progress in Optics XX*, E. Wolf, Ed. Amsterdam, The Netherlands: North-Holland, 1983, pp. 65–153.
- [18] J. B. Khurgin, A. Obeidat, S. J. Lee, and Y. J. Ding, "Cascaded optical nonlinearities: Microscopic understanding as a collective effect," *J. Opt. Soc. Amer. B*, vol. 14, pp. 1977–1983, 1997.
- [19] P. C. Sun, Y. T. Mazurenko, and Y. Fainman, "Real-time one-dimensional coherent imaging through single-mode fibers by space-time conversion processors," *Opt. Lett.*, vol. 22, pp. 1861–1863, 1997.
- [20] A. M. Kan'an and A. M. Weiner, "Efficient time-to-space conversion of femtosecond optical pulses," *J. Opt. Soc. Amer. B*, vol. 15, pp. 1242–1245, 1998.
- [21] J. Janszky, G. Corradi, and R. N. Gyuzalian, "On a possibility of analysing the temporal characteristics of short light pulses," *Opt. Commun.*, vol. 23, pp. 293–298, 1977.
- [22] F. Salin, P. Georges, G. Roger, and A. Brun, "Single-shot measurement of a 52-fs pulse," *Appl. Opt.*, vol. 26, pp. 4528–4531, 1987.
- [23] K. Ema, M. Kuwata-Gonokami, and F. Shimizu, "All-optical sub-Tbits/s serial-to-parallel conversion using excitonic giant nonlinearity," *Appl. Phys. Lett.*, vol. 59, pp. 2799–2801, 1991.
- [24] K. Oba, P.-C. Sun, Y. T. Mazurenko, and Y. Fainman, "Femtosecond single-shot correlation system: A time-domain approach," *Appl. Opt.*, vol. 38, pp. 3810–3817, 1999.
- [25] M. C. Nuss, M. Li, T. H. Chiu, A. M. Weiner, and A. Partovi, "Time-to-space mapping of femtosecond pulses," *Opt. Lett.*, vol. 19, pp. 664–666, 1994.
- [26] T. Feurer, S. Niedermeier, and R. Sauerbrey, "Measuring the temporal intensity of ultrashort laser pulses by the triple correlation," *Appl. Phys. B*, vol. 66, pp. 163–168, 1998.
- [27] D. Mendlovic and A. W. Lohmann, "Space-bandwidth product adaptation and its application to superresolution: Fundamentals," *J. Opt. Soc. Amer. A*, vol. 14, pp. 558–562, 1997.
- [28] T. Konishi and Y. Ichioka, "Ultrafast image transmission by optical time-to-two-dimensional-space-to-time-to-two dimensional space conversion," *J. Opt. Soc. Amer. A*, vol. 16, pp. 1076–1088, 1999.
- [29] A. M. Weiner, D. E. Leaird, D. H. Reitze, and E. G. Paek, "Femtosecond spectral holography," *IEEE J. Quantum Electron.*, vol. 28, pp. 2251–2261, 1992.



Dan M. Marom (S'98–M'01) was born in Detroit, MI, in 1967. He received the B.Sc. and M.Sc. degrees from Tel-Aviv University, Israel, in 1989 and 1995, respectively, and the Ph.D. degree from the University of California, San Diego (UCSD), in 2000.

His doctoral dissertation dealt with femtosecond-rate optical signal processing with applications in ultrafast communications. From 1996 through 2000, he was a Fannie and John Hertz Foundation Graduate Fellow at UCSD. In 2000, he joined Bell Laboratories, Holmdel, NJ, to pursue his

interests in optical communications.

Dr. Marom received the IEEE Lasers and Electro-Optics Society Best Student Paper Award in 1999 for his work describing instantaneous time reversal of complex amplitude ultrafast waveforms.



Dmitriy Panasenکو was born in Moscow, Russia, in 1972. He received the M.Sc. degree from Moscow Institute of Physics and Technology, Russia, in 1995. He is currently pursuing the Ph.D. degree at the University of California, San Diego (UCSD).

He is a Fannie and John Hertz Foundation Graduate Fellow at UCSD. His research interests include ultrashort laser pulse processing and detection techniques and their application to optical communication.

Pang-Chen Sun, photograph and biography not available at the time of publication.

Yuri T. Mazurenko, photograph and biography not available at the time of publication.



Yeshaiahu Fainman (M'93–SM'01) received the Ph.D. degree from Technion—Israel Institute of Technology, Haifa, in 1983.

He is a Professor of Electrical and Computer Engineering at the University of California, San Diego. His current research interests are in nonlinear space-time processes using femtosecond laser pulses for optical communications, near-field phenomena in optical nanostructures, quantum cryptography and communication, 3-D quantitative imaging, and programmable and multifunctional diffractive and

nonlinear optics. He has contributed more than 100 manuscripts to referred journals and more than 170 conference presentations and conference proceedings. He has served on several conference program committees, organized symposiums, and workshops. Currently, he is a Topical Editor of the *Journal of the Optical Society of America A: Optical Signal Processing and Imaging Science*.

Prof. Fainman is a Fellow of the Optical Society of America and SPIE. He received the Miriam and Aharon Gutvirt Prize.